Journal of Alloys and Compounds 509 (2011) 9116–9122

Contents lists available at ScienceDirect

Journal of Alloys and Compounds

journal homepage: www.elsevier.com/locate/jallcom

Morphology and optical properties of Co doped ZnO textured thin films

Tao Wang[a], Yanmei Liu[a,*], Qingqing Fang[a], Yangguang Xu[c], Guang Li[a], Zhaoqi Sun[a], Mingzai Wu[a,b], Junlei Li[a], Hao He[a]

[a] Anhui Provincial Key Laboratory of Information Materials and Devices, Anhui University, Hefei 230039, People's Republic of China
[b] Anhui Key Laboratory of Nanomaterials and Nanotechnology Institute of Solid State Physics Chinese Academy of Sciences, Hefei 230031, People's Republic of China
[c] CAS Key Laboratory of Mechanical Behavior and Design of Materials, Department of Modern Mechanics, University of Science and Technology of China (USTC), Hefei 230027, People's Republic of China

ARTICLE INFO

Article history:
Received 29 April 2011
Received in revised form 15 June 2011
Accepted 15 June 2011
Available online 6 July 2011

Keywords:
Cobalt doped ZnO
Solvothermal
Morphology
Porous
Red-shift
Room-temperature ferromagnetic

ABSTRACT

Depending on the ZnO seed-layers, a new kind of cobalt doped zinc oxide ($Zn_{1-x}Co_xO$) thin films with controllable morphology were prepared by a facile solvothermal method. A series of ZnO thin films with different Co contents were applied to study the effect of doped Co on morphology, structural and optical properties. It is found that the doped content plays an important role on morphology evolution of $Zn_{1-x}Co_xO$ films. The results of scanning electron microscope (SEM) indicate that the $Zn_{1-x}Co_xO$ films are highly uniform and porous. Co has been successfully doped into the ZnO lattice structure and revealed by X-ray diffraction (XRD) and energy dispersive spectrum (EDS). It can be found that $Zn_{1-x}Co_xO$ thin films possess good crystalline quality through the characterization of transmission electron microscope (TEM) and high-resolution transmission electron microscopy (HRTEM). All of the samples show a stronger violet emission and ultraviolet absorption, and the violet emission peaks shift towards red with increasing of Co content. In addition, the magnetic result demonstrates that the prepared Co-doped ZnO thin films are room-temperature ferromagnetic materials.

1. Introduction

Morphology design and doping have been the main means to improve the performance of materials. Over the past few years, extended and oriented nanostructures are desirable for many applications, but direct fabrication of complex nanostructures with controlled crystalline morphology, orientation and surface architectures remains a great challenge [1]. With the discovery of carbon nanotubes, one-dimensional (1D) nanomaterials have attracted a great deal of interest. However, two-dimensional nanosheets are regarded as a new class of nanostructured materials in recent years due to their high anisotropy, nanometer-scale thickness and possessing interesting properties [2,3], and have wide applications in many fields. In this case, many chemists and material scientists have been exploiting their synthetic routes [4].

Doping of semiconductors by impurity atoms achieved their widespread technological applications in microelectronics and optoelectronics [5], and nanocrystals doped with magnetic impurities are of interest for their potential use in spin-based electronic devices [6]. On this account, diluted magnetic semiconductors (DMSs) have caused extensive scientific concerns because of their potential applications in spintronics and optoelectronics [7–9]. Most of these materials are obtained from various wide-band-gap semiconductors doped with transition-metal (TM) ions. Initiated by theoretical predictions [10,11], 3d-transition-metals (TM)-doped ZnO would be a good candidate to achieve Curie temperature above room temperature. Therefore, cobalt and other transition metal (TM) elements doped ZnO nanomaterials have become a focus for many researchers. However, among numerous reports on $Zn_{1-x}Co_xO$ thin films, very few have been published on morphology design of thin films, which is of special interest as building blocks for the applications of DMSs, such as spintronic, electro-optical devices and microwave absorbing materials.

How to design the morphology of doped nanocrystal to better control performance of materials is always an important task. Here, we report on the synthesis of cobalt doped zinc oxide ($Zn_{1-x}Co_xO$) textured thin films on glass substrate by solvothermal method. Homogeneous nucleation processes can be obtained by this method, and it also can reduce stoichiometry problems associated with the volatilization of high-vapor pressure components [12]. We found that the doped content has significant impact on the morphology of $Zn_{1-x}Co_xO$ thin films. When the doped content is lower than 20%, the prepared $Zn_{1-x}Co_xO$ thin films display highly uniform and porous morphology. Co is successfully doped into the ZnO wurtzite lattice structure as revealed by X-ray

* Corresponding author. Tel.: +86 5515107284; fax: +86 5515107237.
E-mail addresses: Wang_shu_guang@163.com (T. Wang), taowang166@gmail.com (Y. Liu).

0925-8388/$ – see front matter © 2011 Elsevier B.V. All rights reserved.
doi:10.1016/j.jallcom.2011.06.066

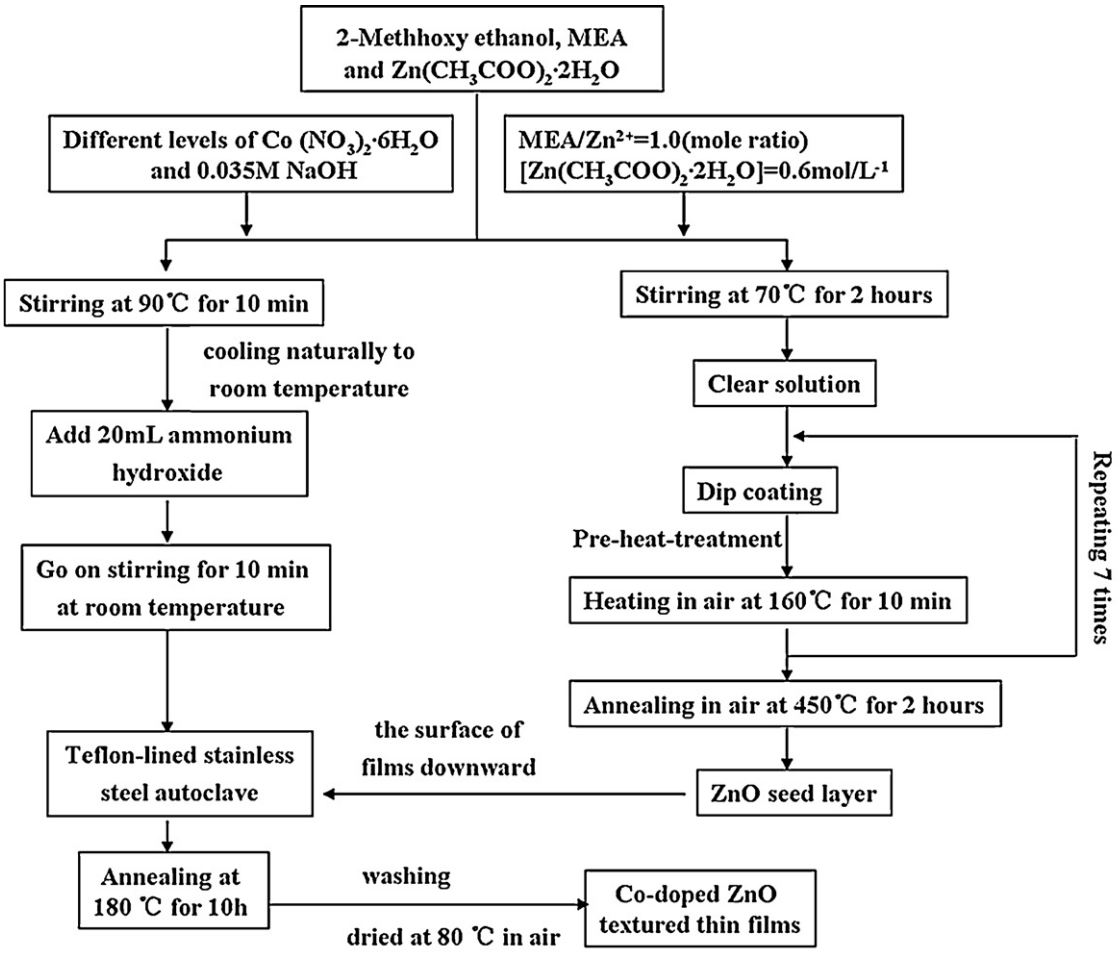

Fig. 1. Schematic illustration of the procedure for preparing $Zn_{1-x}Co_xO$ textured thin films.

diffraction (XRD) and verified by the energy dispersive spectrum (EDS). The doping effect of ZnO on structural and optical properties is investigated. The vibrating sample magnetometer (VSM) shows that $Zn_{1-x}Co_xO$ textured films have distinct room-temperature ferromagnetic behavior. This novel nanostructure is suggested to have important applications in microwave absorbing and spintronic devices.

2. Experimental methods

All chemicals are analytical grade and purchased from Jin Chang New Material Company. The detailed flowchart which shows the procedure used for preparing $Zn_{1-x}Co_xO$ textured thin films is shown in Fig. 1. Pure ZnO thin films were prepared by sol–gel technology on glass substrates and employed as seed layers to further develop into $Zn_{1-x}Co_xO$ films. The thickness of seed layers was approximately 250 nm. After spin-coating, the seed layers were placed in muffle furnace and annealed at 450 °C for 2 h.

In the hydrothermal process, the precursor solution consists of 0.05 M zinc acetate dihydrate ($Zn(AC)_2{\cdot}2H_2O$), 0.035 M sodium hydroxide (NaOH) and different contents of cobalt nitrate hexahydrate ($Co(NO_3)_2{\cdot}6H_2O$) dissolved in 2-methhoxy ethanol. 0.05 M monoethanol amine (MEA) was then added to the mixture, the mixture was stirred at 90 °C for 10 min until milky and saturated liquid appeared, and then cooled naturally to room temperature. 20 mL ammonium hydroxide ($NH_3{\cdot}H_2O$) was added to the mixture and continued to be stirred for 10 min at room temperature. Finally, the mixture was added into a Teflon-lined stainless steel autoclave, and then the spin coating films placed and facing downward in the growth solution, sealed and maintained at 180 °C for 10 h. After the autoclave was cooled naturally to room temperature, the resulting films were taken out and washed with deionized water followed by ethanol to remove ions possibly remaining in the final product, and then dried at 80 °C in air for further characterization.

The surface morphology of $Zn_{1-x}Co_xO$ thin films was examined by using a scanning electron microscope (SEM Sirion200). Structural analysis of the thin films was carried out with X-ray diffraction (XRD MAP18AHF) via Cu Ka line at the excitation voltage of 40 kV and tube current of 100 mA. The composition of films was obtained via energy-dispersive X-ray (EDX) spectrum analysis. High-resolution transmission electron microscopy (HRTEM, JEOL-2010) was used to investigate the morphology, composition, and microstructure of $Zn_{1-x}Co_xO$. The photoluminescence (PL LABRA-HR) were measured under the excitation of xenon lamp laser (325 nm) at room temperature. The optical transmittance of the films was measured by a U-4100 Spectrophotometer (Liquid) in the wavelength range from 240 to 800 nm. Magnetic hysteresis loops were measured by a vibrating sample magnetometer (VSM, BHV-55) at room temperature.

3. Results and discussion

This study focuses on the influence of different Co doping on morphology evolution, structural, and optical properties of the obtained thin films. The textured thin films were synthesized by reacting $Zn(AC)_2{\cdot}2H_2O$ and different contents of dopant precursor ($Co(NO_3)_2{\cdot}6H_2O$) depending on the ZnO seed layers. The surface color of synthesized thin films is green.

The SEM images of $Zn_{1-x}Co_xO$ textured thin films are shown in Fig. 2. It can be obviously found that the surface morphology of films is affected vitally by doped Co content. When the doped content of Co is 5%, a large area of flowerlike structures can be observed. These connected flowerlike structures are composed of nanosheets. The major part of these nanosheets stands on the substrate, whose edges pointing each other with a little angle. The thickness of nanosheets is about 10–20 nm. Such special morphology provides necessary surface roughness as well as a highly porous two-dimensional structure to our later film functionalization. With

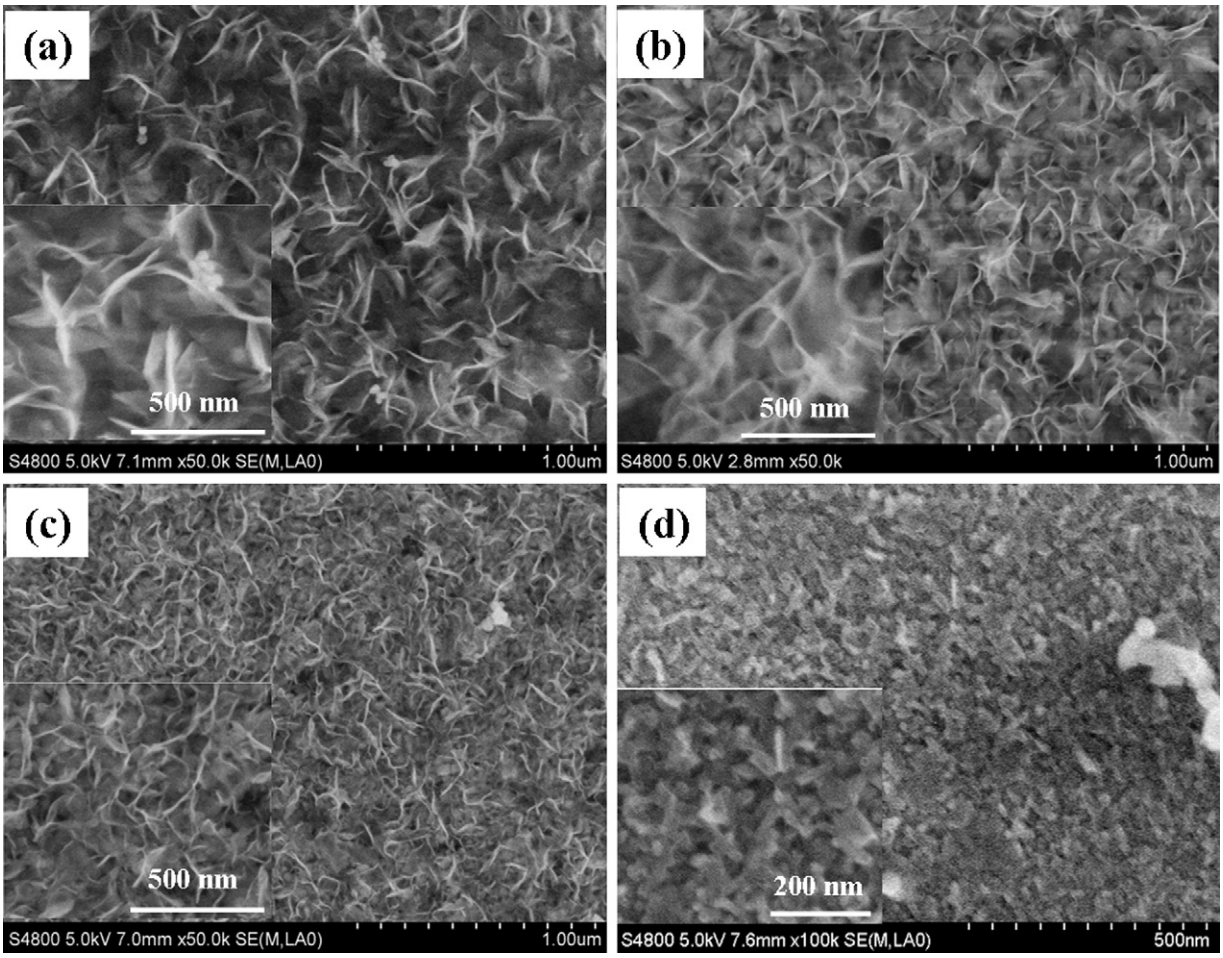

Fig. 2. SEM images of fabricated $Zn_{1-x}Co_xO$ textured thin films: (a) $Zn_{0.95}Co_{0.05}O$; (b) $Zn_{0.9}Co_{0.1}O$; (c) $Zn_{0.85}Co_{0.15}O$; (d) $Zn_{0.8}Co_{0.2}O$.

the increasing of Co content, nanosheets turn to be smaller and the texture structure is denser (Fig. 2b and c). When the Co content reaches 20%, the texture structure has disappeared and replaced by a layer of small and compact nanorods on the surface of the film (Fig. 2d). The length of nanorods is about tens of nanometer.

Further morphology characterization and structural analysis of $Zn_{1-x}Co_xO$ films were performed by TEM. Fig. 3 shows typical TEM images of $Zn_{1-x}Co_xO$ textured thin films. Detailed observation from the TEM images (Fig. 3a and b) clearly confirms the rough surface and high porosity of $Zn_{1-x}Co_xO$ thin film. Fig. 3c and d are HRTEM images of $Zn_{1-x}Co_xO$ thin film, and the inset of Fig. 3d is the corresponding SAED pattern. These results indicate that the sample is highly crystalline without any impurity phases, and has a wurtzite structure. Besides, from the magnified HRTEM images, the lattice spacing is measured around 0.24 nm, which corresponds to the $[1\,0\,\bar{1}\,1]$ direction of hexagonal ZnO, this suggests that one of the growth directions of the ZnO nanoentities is along the $[1\,0\,\bar{1}\,1]$.

X-ray diffraction (XRD) patterns shown in Fig. 4 are recorded for the analysis on the crystal phase of ZnO textured thin films with different doped contents. The XRD results reveal that all the diffraction peaks can be indexed to the wurtzite structure of ZnO (space group *P*63*mc*) and no characteristic peaks from impurities are detected within experimental error, which indicates possible doping throughout the nanostructure. The three most intense peaks of the XRD pattern of $Zn_{1-x}Co_xO$ samples are clearly shown in Fig. 4a, from left of which are (1 0 0), (0 0 2), and (1 0 1) diffraction peaks of ZnO, respectively. It is worth mentioning that (1 0 1) peaks of all samples show shifting slightly towards higher angle by increasing the contents of Co^{2+} (as shown in Fig. 4b), which indicates a reduction of the unit cell due to Co^{2+} substitution in ZnO lattices. This is supported by the fact that the ionic radius of Co^{2+} is 0.72 Å whereas that of Zn^{2+} is 0.74 Å [13]. The shifting of XRD lines strongly suggests that Co^{2+} is successfully substituted into the ZnO structure at the Zn^{2+} site.

To precisely examine the chemical composition of $Zn_{1-x}Co_xO$ thin films, energy dispersive spectrum (EDS) was performed without the interference from the substrate. Fig. 5 shows the EDS spectra of $Zn_{0.8}Co_{0.2}O$, and the Co peak is clearly shown in the EDS spectra, which suggests that Co^{2+} has successfully doped in the lattice of ZnO. The Co content in the ZnO film is determined 18.0 at.%. Obviously, the amount of Co incorporated into the ZnO matrix is less than that provided in the reaction solution. This may be because the bond energy of Co–O is higher than that of Zn–O, and more energy is required to enable Co^{2+} to enter the lattice and form the Co–O bond. Therefore, Co^{2+} substituting for Zn^{2+} qualifies a higher stability than the Zn–O structure, and more energy is required in the substituted samples to form the Zn–O–Co structure.

Fig. 6 depicts the room-temperature photoluminescence (PL) spectrum of $Zn_{1-x}Co_xO$ textured thin films with different Co contents, which is an effective method for the investigation of intrinsic point defects in ZnO, such as zinc vacancies, interstitial oxygen, interstitial zinc, and oxygen vacancies [14]. As shown in Fig. 6, all samples exhibit a strong UV emission at near 400 nm and two relatively weak emission bands center at 470 and 530 nm. The UV luminescence band belongs to the exciton recombination corresponding to near-band-edge emission of the $Zn_{1-x}Co_xO$ films [15].

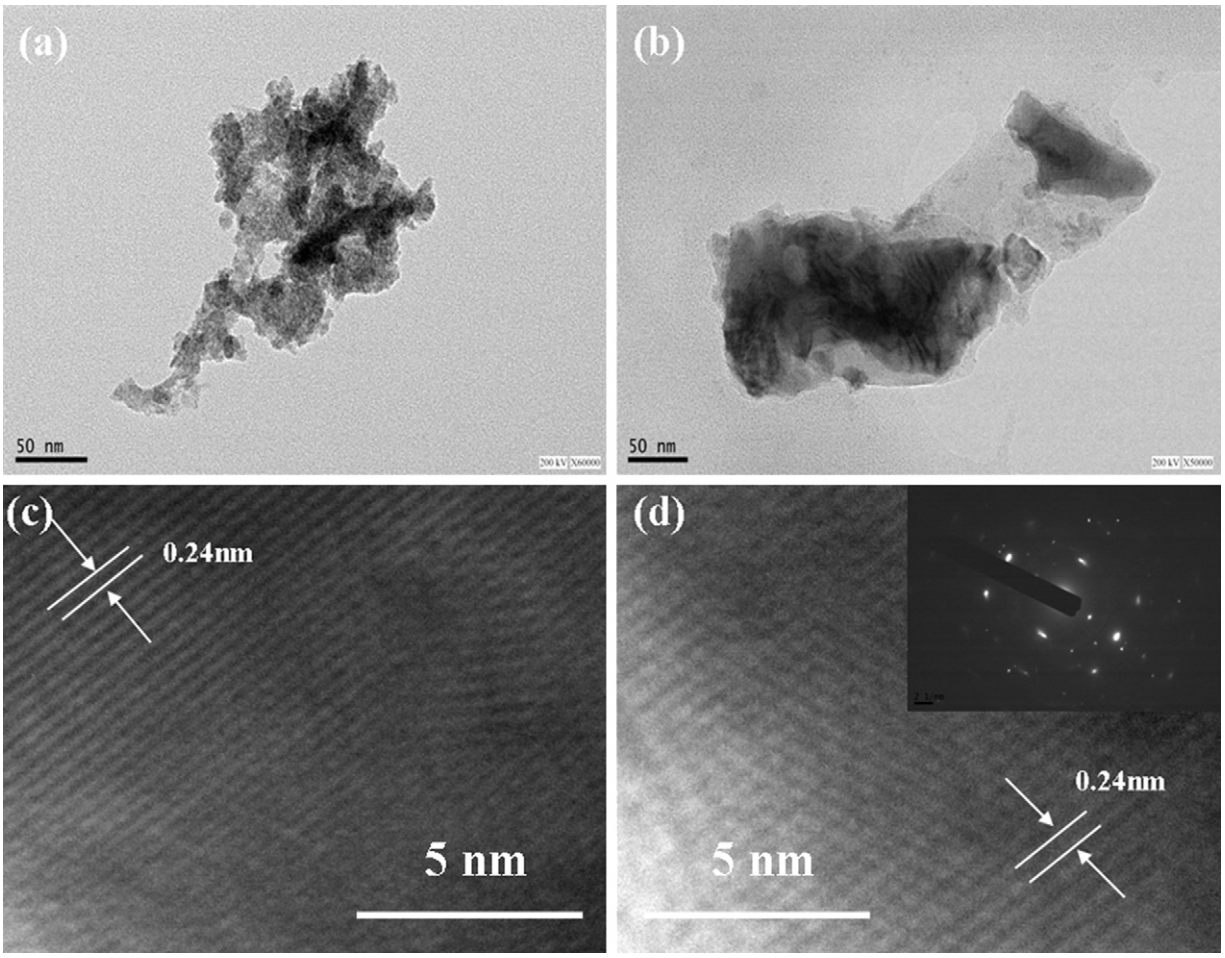

Fig. 3. (a) and (b) TEM images of $Zn_{1-x}Co_xO$ thin film; (c) and (d) HRTEM images of $Zn_{1-x}Co_xO$ thin film, and the inset of (d) is the corresponding SAED pattern.

The position of each sample's UV-emission peak is marked in the spectra, and it can be clearly observed that the UV-emission peaks generate red-shift phenomenon. This could mainly due to the sp–d exchange interactions between the band electrons and the localized d electrons of the Co^{2+} ions substituting Zn ions [16–18]. This sp–d exchange interaction is verified by the observation of a strong magneto-optical effect near the band gap region of $Zn_{1-x}Co_xO$ alloys [19]. The s–d and p–d exchange interactions cause a negative and a positive correction to the conduction and valence band edges, respectively, which therefore leads to band gap narrowing [20]. Besides, the intensity of UV emission decreases successively with the concentration of Co^{2+} increasing from 5% to 15%. This may be because more defect states below the conduction band occurs via Co doping, so that some of the exited electrons in the conduction band relax to the defect states which leads to decreasing in UV emission intensity [21]. The weak peak at 470 nm is blue emission, Zeng et al. [22] reported that it can be attributed to the transition from extended Zn_i states. The extended Zn_i states are slightly below

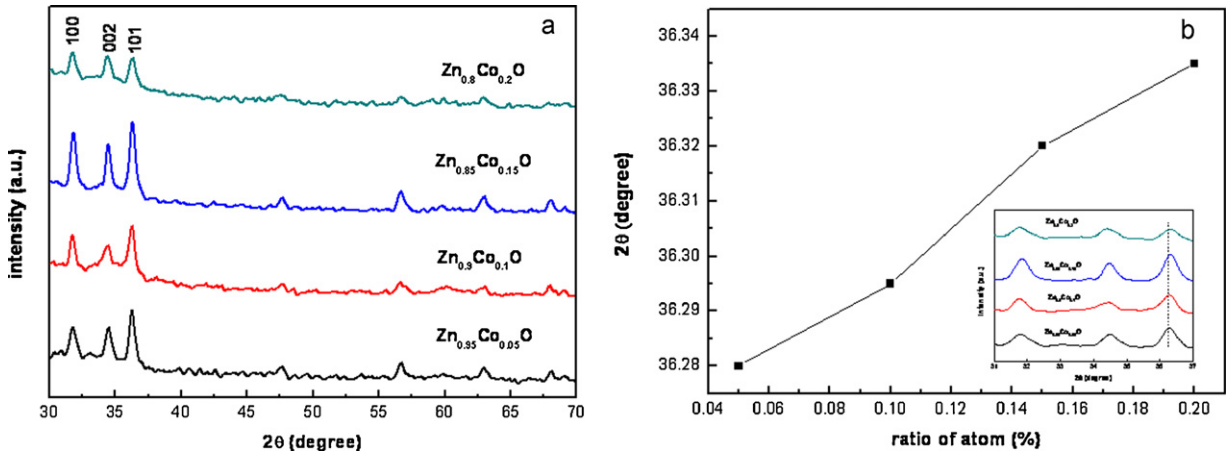

Fig. 4. (a) XRD patterns taken from the $Zn_{1-x}Co_xO$ textured thin films with different doping content; (b) the position of (0 0 2) diffraction peak of different films; inset of (b) shows shift of the center of (0 0 2) diffraction peak.

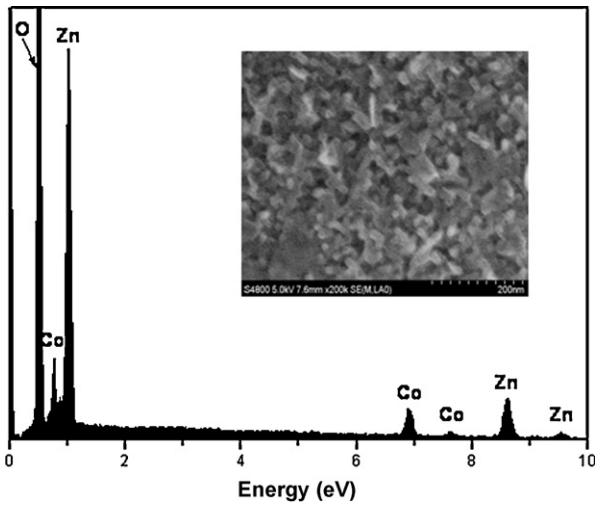

Fig. 5. EDS of a Co:ZnO textured thin film ($Zn_{0.8}Co_{0.2}O$).

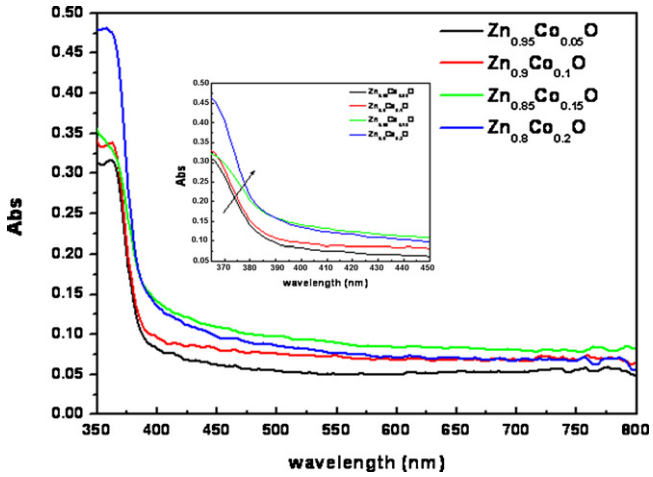

Fig. 7. Absorbance spectra of different $Zn_{1-x}Co_xO$ thin films.

the simple Zn_i state, to the valance band. These extended states can be formed during the annealing process according to the defect ionization reaction, and can result in defect localization coupled with a disordered lattice. The electrons can first transit to the conduction band or Zn_i state, then relax to extended Zn_i states, and finally transit to the valance band with blue emission. The green emission at 530 nm is usually caused by the transition of a photogenerated electron [23].

Fig. 7 shows the UV–vis absorption spectra collected from different $Zn_{1-x}Co_xO$ thin films. The strong absorption band between 375 and 385 nm (characteristic of the wide-band semiconductor material) originates from ZnO. From the inset of Fig. 7, we can find that the absorption edges shift to long wavelength (red-shift). The red shift phenomenon can be explained by the Burstein–Moss band gap widening and band gap narrowing due to the electron–electron and electron-impurity scattering [24].

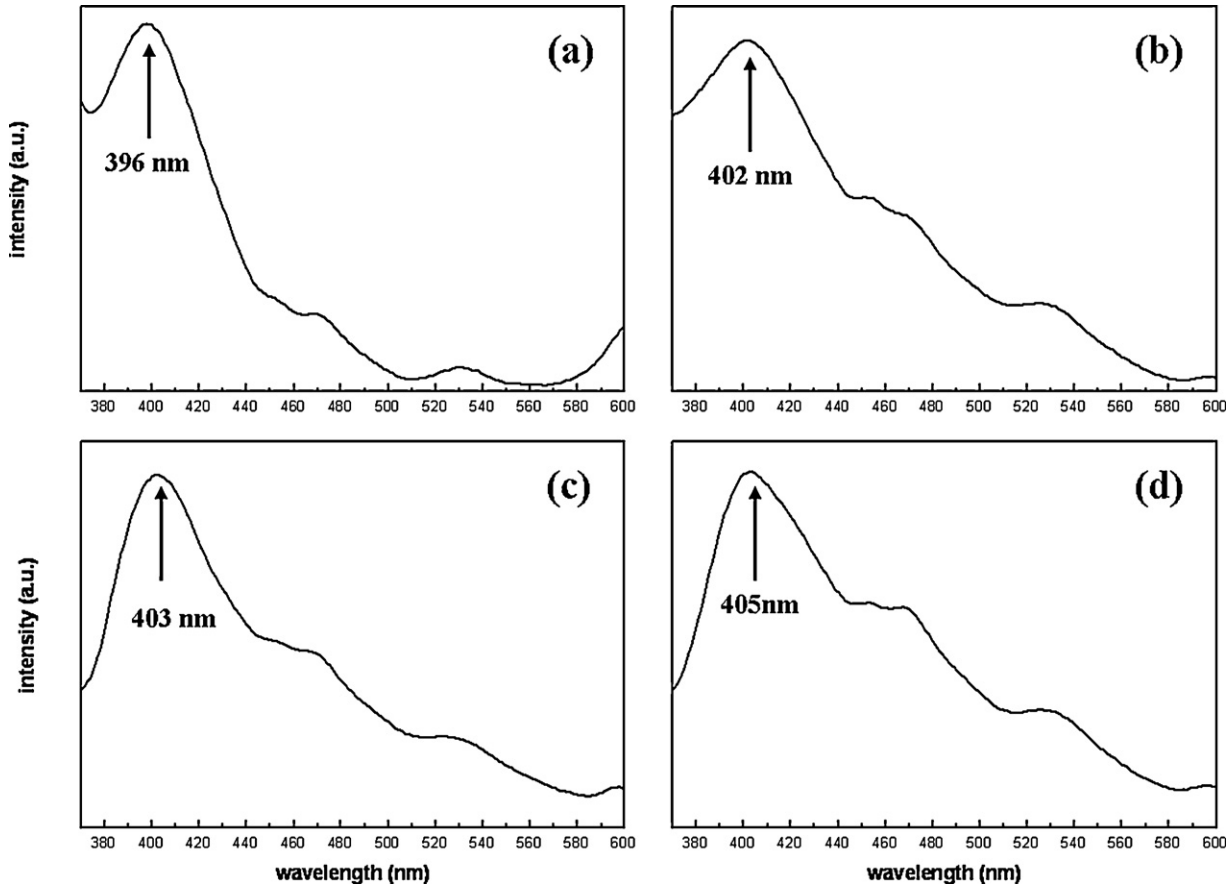

Fig. 6. Room-temperature PL spectrum of $Zn_{1-x}Co_xO$ textured thin films with different Co contents: (a) $Zn_{0.95}Co_{0.05}O$; (b) $Zn_{0.9}Co_{0.1}O$; (c) $Zn_{0.85}Co_{0.15}O$; (d) $Zn_{0.8}Co_{0.2}O$.

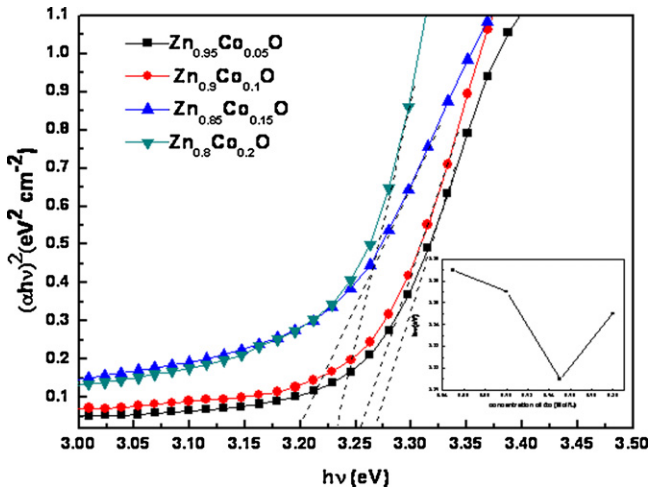

Fig. 8. Plots of $(\alpha h\nu)^2$ against $h\nu$ for different $Zn_{1-x}Co_xO$ thin films.

In order to determine the optical band gap energy E_g from the absorption spectra, we used the variation of the absorption coefficient (α) with photon energy, the equation is as follows [25]:

$$(\alpha h\nu) = A(h\nu - E_g)^{1/2} \quad (1)$$

where E_g is the optical band gap of the films and A is constant. Fig. 8 shows the plots of $(\alpha h\nu)^2$ versus $(h\nu)$ for the various $Zn_{1-x}Co_xO$ thin films. The calculated band gap value of Co doped ZnO thin films are found to be from 3.26 to 3.20 eV. The variation of band gap with the concentration of Co is shown in the inset of Fig. 8, in which it can be found that the E_g decreases with increasing of Co content except for the sample of $Zn_{0.8}Co_{0.2}O$. This is because the band filling effect (Burstein–Moss effect), overcompensates the band-gap renormalization effect due to heavy doping [26].

The magnetic property of $Zn_{0.85}Co_{0.15}O$ is shown in Fig. 9. The applied field range is −2500 to 2500 Oe. The sample exhibits well-defined hysteresis loops at 300 K. Fig. 9 reveals that the coercive field is 230 Oe. The origin of ferromagnetism in doped semiconductor oxide materials has been controversial, while structural defects and magnetic impurities have often been invoked to explain magnetic ordering [27–29]. Here, the cause of ferromagnetic behavior

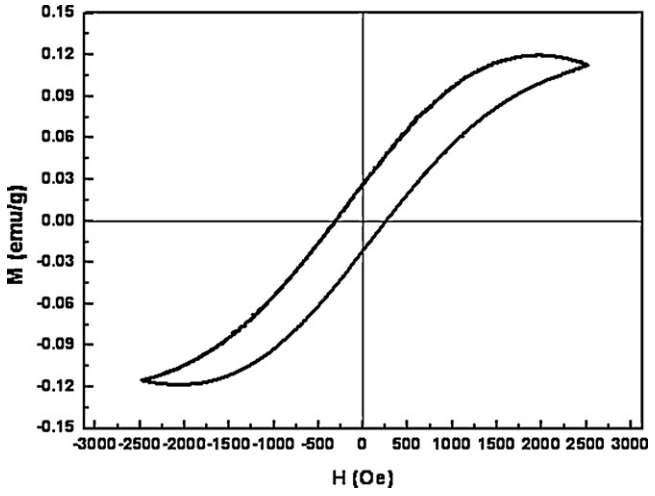

Fig. 9. Room temperature magnetic hysteresis loops (M–H curve) for the $Zn_{0.85}Co_{0.15}O$ sample.

in the system should be the substitution of Co^{2+} ions in ZnO lattice. A weak ferromagnetic behavior suggests that the content of cobalt ions in the ZnO lattice is not enough.

4. Conclusions

In summary, a new and large-scale two-dimensional $Zn_{1-x}Co_xO$ flowerlike thin film has been prepared by a facile solvothermal method. It has been found that the doped contents of Co have great influence on the morphology, structural and optical properties of $Zn_{1-x}Co_xO$ films. The $Zn_{1-x}Co_xO$ thin films show stronger UV emission and the position of each sample's UV-emission peak shift towards long wave (red-shift). The absorption edges of all samples generate red-shift phenomenon. The result of X-ray diffraction (XRD) and energy dispersive spectrum (EDS) indicate that cobalt is successfully doped into the ZnO wurtzite lattice structure, and no secondary magnetic phases are found. A typical room-temperature ferromagnetic behavior has been found in $Zn_{1-x}Co_xO$ flowerlike films, it suggests that the solid solution of Co ions in ZnO thin films plays a major role in production of observed ferromagnetic properties. Prospectively speaking, this work not only obtains the morphology-controllable $Zn_{1-x}Co_xO$ films, but also proposes an effective and simple way to tailor morphologies of inorganic materials for the potential applications. Further investigation on the Co doped ZnO textured thin films will be published in future articles.

Acknowledgements

The work is supported by Anhui Provincial Key Laboratory of Information Materials and Devices, the Anhui Provincial Natural Science Fund (090414177), the National Science Foundation of China (50872001), the National Science Foundation of China (51072001), Scientific Research Startup Outlay for Doctors in Anhui University and the Anhui Provincial second Fifteen Fund for Middle-aged and Young outstanding teachers in the province of colleges and universities (211).

References

[1] R. Zheng, R. Tian, J.A. Voigt, J. Liu, B. Mckenzie, M.J. Mcdermott, M.A. Rodriguez, H. Konishi, H.F. Xu, Nat. Mater. 2 (2003) 821–826.
[2] T. Sasaki, Y. Ebina, Y. Kitami, M. Watanabe, J. Phys. Chem. B 105 (2001) 6116.
[3] J.Q. Hu, Y. Bando, J.H. Zhan, Y.B. Li, T. Sekiguchi, Appl. Phys. Lett. 83 (2003) 4414.
[4] S. Park, J.H. Lim, S.W. Chung, C.A. Mirkin, Science 303 (2004) 348–351.
[5] D. Mocatta, G. Cohen, J. Schattner, O. Millo, E. Rabani, E. Rabani, U. Banin, Science 1 (2011) 332.
[6] R. Beaulac, L. Schneider, P.I. Archer, G. Bacher, D.R. Gamelin, Science 325 (2009) 973.
[7] J.M.D. Coey, M. Venkatesan, C.B. Fitzgerald, Nat. Mater. 4 (2005) 173.
[8] T. Dietl, H. Ohno, F. Matsukura, J. Cibert, D. Ferrand, Science 287 (2000) 1019.
[9] S.A. Wolf, D.D. Awschalom, R.A. Buhrman, J.M. Daughton, S. von Molnár, M.L. Roukes, A.Y. Chtchelkanova, D.M. Treger, Science 294 (2001) 1488.
[10] K. Sato, H. Katayama-Yoshida, Jpn. J. Appl. Phys. 39 (2000) L555.
[11] K. Sato, H. Katayama-Yoshida, J. Appl. Phys. 40 (2001) L334.
[12] S.H. Yu, J. Ceram. Soc. Jpn. 109 (2001) 65–75.
[13] M.A. Hemet, N. Nagasljndaramd, A.H. Kreszowski, Phys. Chem. Solid 51 (1990) 12.
[14] Y.C. Qiu, W. Chen, S.H. Yang, B. Zhang, X.X. Zhang, Y.C. Zhong, K.S. Wong, Cryst. Growth Des. 10 (2010) 1.
[15] J.J. Wu, S.C. Liu, Adv. Mater. 14 (2002) 215.
[16] J. Diouri, J.P. Lascaray, M. Amrani, Phys. Rev. B 31 (1985) 7995.
[17] R.B. Bylsma, W.M. Becker, J. Kossut, U. Debska, D. Yoder-Short, Phys. Rev. B 33 (1986) 8207–8215.
[18] Y.D. Kim, S.L. Cooper, M.V. Klein, B.T. Jonker, Phys. Rev. B 49 (1994) 1732–1742.
[19] K. Ando, H. Saito, Z. Jin, T. Fukumura, M. Kawasaki, Y. Matsumoto, H. Koinuma, Appl. Phys. Lett. 78 (2001) 2700–2702.
[20] Y.R. Lee, A.K. Ramdas, R.L. Aggarwal, Phys. Rev. B 38 (1988) 10600.

[21] A.H. Wang, B.L. Zhang, X.C. Wang, N. Yao, Z.F. Gao, Y.K. Ma, L. Zhang, H.Z. Ma, J. Phys. D: Appl. Phys. 41 (2008) 215308.
[22] H.B. Zeng, G.T. Duan, Y. Li, S.K. Yang, X.X. Xu, W.P. Cai, Adv. Funct. Mater. 20 (2010) 561–572.
[23] K. Vanheusden, W.L. Warren, C.H. Seager, D.R. Tallant, J.A. Voigt, B.E. Gnade, J. Appl. Phys. 79 (1996) 7983.
[24] B. Joseph, P.K. Manoj, V.K. Vaidyah, Ceram. Int. 32 (2006) 487–493.
[25] E. Bacaksiz, S. Aksu, B.M. Baso, M. Altunbaş, M. Parlak, E. Yanmaz, Thin Solid Films 516 (2008) 7899–7902.
[26] B.E. Sernelius, K.F. Berggren, Z.C. Jin, I. Hamberg, C.G. Granqvist, Phys. Rev. B 37 (1988) 10244.
[27] M. Venkatesan, C.B. Fitzgerald, J.G. Lunney, J.M.D. Coey, Phys. Rev. Lett. 93 (2004) 177206.
[28] A. Sundaresan, R. Bhargavi, N. Rangarajan, U. Siddesh, C.N.R. Rao, Phys. Rev. B 74 (2006) 161306(R).
[29] J.B. Yi, H. Pan, J.Y. Lin, J. Ding, Y.P. Feng, S. Thongmee, T. Liu, H. Gong, L. Wang, Adv. Mater. 20 (2008) 1170.